

Hierarchical, Hybrid Framework for Collision Avoidance Algorithms in the National Airspace*

Michael P. Vitus[†] Claire J. Tomlin[‡]

In this paper, a hierarchical, hybrid framework is proposed for representing and analyzing the interaction of multiple aircraft operating under different collision avoidance and separation assurance regimes. The model is broken down by the three different collision avoidance regimes: immediate collision avoidance, midterm collision avoidance and separation assurance. These schemes are classified by the time scale in which they operate. Even though each collision avoidance scheme is independently safe, when they are combined the entire system can become unsafe. In this paper, backwards reachable sets are used to analyze the interaction between the immediate and midterm collision avoidance schemes resulting in provable safety conditions. The vertical reachable set is also used to analyze the Traffic Alert and Collision Avoidance System (TCAS), a specific immediate collision avoidance scheme.

I. Introduction

The goal of the Next Generation Air Transportation System (NGATS) is to increase the capacity of the National AirSpace (NAS) while increasing the efficiency and safety of the airspace. Currently, there are many collision avoidance algorithms that exist or are being developed for different time scales.¹⁻⁹ Even though each individual algorithm may provide safety between the aircraft, when combined to form a hybrid collision avoidance system for all time scales, safety cannot be guaranteed. Therefore to facilitate NGATS, methods need to be developed for analyzing the interaction between airborne collision avoidance systems and tactical separation assurance tools in Air Traffic Control (ATC). Furthermore, procedures need to be designed to guarantee that these collision avoidance and separation assurance tools do not conflict with each other, but rather operate together safely and efficiently. This interoperability of collision avoidance functions is integral to the design of NGATS. In the proposed approach, reachable set analysis is used to obtain a provable safety guarantee. The reachable set analysis used considers pairs of aircraft which is a limitation in a multi-aircraft encounter, however many existing collision avoidance algorithms are only designed for pairs of aircraft.

Collision avoidance systems can generally be classified into three groups according to the time horizons over which they operate. Current airborne collision avoidance schemes, such as the Traffic Alert and Collision Avoidance System (TCAS), operate over a time horizon of less than a minute. These schemes will be denoted as immediate collision avoidance schemes. New automated methods for both ground-based and airborne collision avoidance are being designed for a time horizon of a few minutes, denoted as midterm collision avoidance schemes. Finally, tactical air traffic control schemes provide separation to aircraft over a longer time horizon of about 30 minutes. These are denoted as separation assurance schemes. Within these three groups, the methods may be further classified according to their ability to treat pairwise or multiple (more than 2) aircraft conflicts. Because the NGATS will involve simultaneous operation of, and switching between, multiple collision avoidance and separation assurance schemes, it is imperative to ensure that the interoperation of these schemes results in safe air traffic management (ATM). Second, it is important to understand the performance of ATM when switching between these schemes, especially in high density

*This research was supported by the NASA grant NNA06CN22A

[†]Ph.D. Candidate, Department of Aeronautics and Astronautics, Stanford University. AIAA Student Member. vitus@stanford.edu

[‡]Professor, Department of Electrical Engineering and Computer Sciences, University of California at Berkeley. Research Professor, Department of Aeronautics and Astronautics; Director, Hybrid Systems Laboratory, Stanford University. AIAA Member. tomlin@stanford.edu

situations with multiple potential aircraft conflicts. Currently, there is no framework for analyzing the interaction between different collision avoidance schemes.

A hierarchical, hybrid model is proposed for representing and analyzing the interaction of multiple aircraft operating under the collision avoidance and separation assurance regimes. The framework is shown in Figure 1, and will be used to represent interactions in a region of airspace, either enroute or terminal, comprising of a few sectors (such that the total time taken to traverse the region is about 30 minutes).

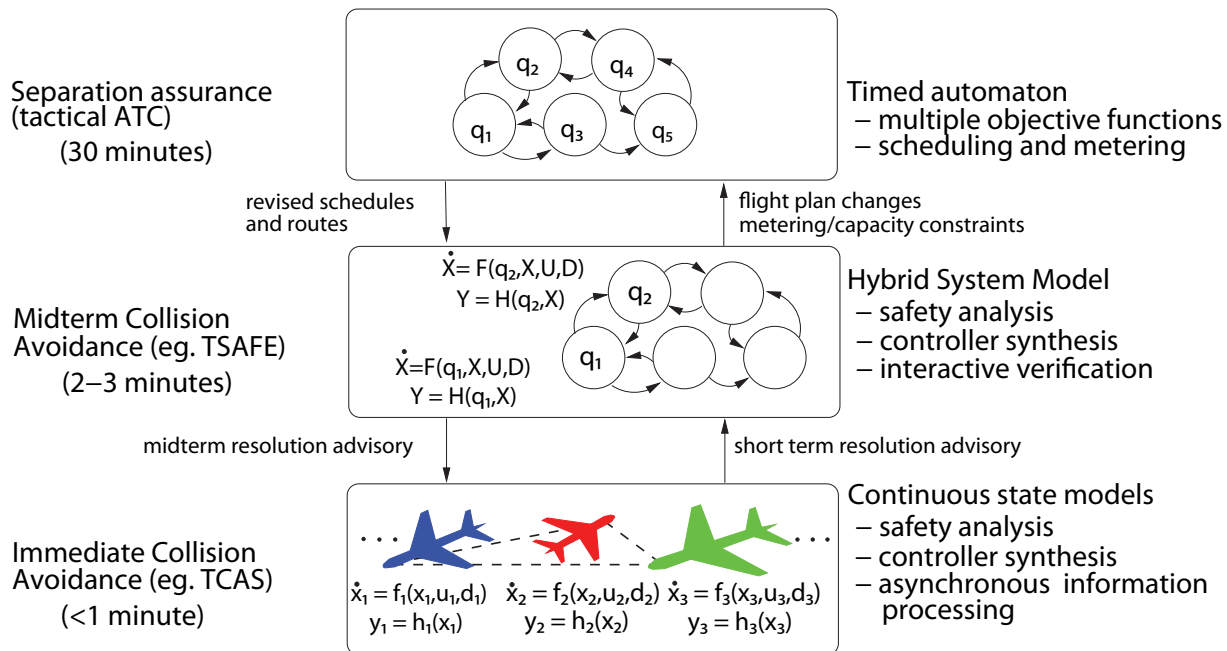


Figure 1. A hierarchical, hybrid system representation of the interaction between the immediate collision avoidance regime (continuous models), the midterm collision avoidance regime (hybrid models), and the separation assurance regime (timed automata).

II. System Model

The hierarchical, hybrid system model is broken down by the three different collision avoidance regimes: immediate, midterm and tactical. Switching can occur between these states due to flight plan changes, revised routes, and resolution advisories. This section will go into more detail on each of the three regimes.

A. Immediate Collision Avoidance regime

At the lowest level of the hierarchy is the immediate collision avoidance regime, in which airborne collision avoidance schemes are in effect over a time horizon of less than one minute. TCAS is an example of such a scheme. Due to the short time horizon and small relative distances between aircraft, it is important at this level of abstraction to correctly model the dynamics and maneuvering capability of each aircraft involved. Thus, each aircraft is represented with a continuous-state dynamic model $\dot{x}_i = f_i(x_i, u_i, d_i)$ (for aircraft i) with state variables x_i , control inputs u_i , and disturbances d_i , as shown in Figure 1. The state variables could represent the position, orientation and velocities of the aircraft, the inputs could be thrust, angle of attack and angular velocities, and disturbances represent environmental uncertainties such as the effect of wind and weather, over which one has no control. Sensor measurements of the state variables of each system are represented by the output functions h_i . Also, it is desirable to consider both deterministic and stochastic sources of uncertainty into the system. Deterministic uncertainty is represented as worst case bounds on disturbances, such as the effects of wind on the aircraft velocities. Stochastic uncertainty is represented using probabilistic data fields for weather.

The aircraft are assumed to be in communication with each other and with ATC, and while the data may be time stamped (eg. GPS provides very accurate clock values which may be tagged to each data packet), potentially causing each vehicle to receive information for its next control action at different times.

B. Midterm Collision Avoidance regime

The middle layer of the hierarchy represents an abstraction of the immediate collision avoidance layer. Since this layer models aircraft interaction over a longer time horizon than the previous, it is sufficient to use simpler models to represent the motion of each individual aircraft. These could be, for example, kinematic models representing each aircraft as a point moving through the airspace in response to simple changes in aircraft speed or direction,^{6,10,11} for example, flying along straight lines or arcs of circles.^{7,12} Such models are amenable to fairly simple representations of group behavior. A key feature of the models at this layer is that they are hybrid: there is a finite set of discrete states representing the set of possible behaviors or configurations of an aircraft or a group of aircraft; then associated to each of these discrete states, or modes, are the relative kinematics of the aircraft in that state. For example, in Figure 1, the discrete state q_1 could represent that the group of aircraft within a given region satisfies the minimum separation requirements. The switch to q_2 could represent an unforeseen circumstance in which a new aircraft enters the region, causing separation standards to be violated. The system could then switch to another airborne collision avoidance control law. In each mode, the relative kinematics of the aircraft motion is represented as $\dot{X} = F(q_i, X, U, D)$, where the state is mixed discrete-continuous (q_i, X) , with corresponding grouped inputs and disturbances (U, D) . All states are not assumed to be observable, and thus are also represented by the output function $H(q_i, X)$ in each state.

C. Separation Assurance regime

At the top of the hierarchy is a timed automaton model¹³ of the system. This model abstracts the aggregate behavior of the continuous systems into discrete modes of operation q_i . The transition logic between modes is easily understandable and controllable by a central authority (ATC) overseeing the operation of the system. Here, the modes may be representative of system configurations describing: the state of occupancy of sectors and level of congestion, weather state, closure of a region of airspace, miles-in-trail constraint along a jetway, and other constraints. The modes can also represent the controlled state of the aircraft, as in the example shown in Figure 2.¹⁴ Generally the aircraft flies at constant heading at the average speed for the type of aircraft at a given altitude. ATC will typically enforce separation constraints by commanding the aircraft to slow down or speed up (to within 10% of its average speed), or will impose a path deviation on the aircraft such as a detour, shortcut, vector for spacing (VFS), or altitude change. As a last resort, the aircraft will be put into a holding pattern. Associated to each mode, the continuous dynamics may be abstracted into simple timers, representing a clock. These clocks can be reset when switching from mode to mode, and the values of the clocks can be used as guards to control the transition from one state to another. These models are appropriate for tactical level control: they provide an abstract representation, for example, of graph theoretic flow models¹⁵ which are used to represent metering-scheduling problems at time horizons of up to 30 minutes.

D. Hybrid System

Intuitively, the incorporation of controlled switches from one mode to another can allow the system to switch to safety in another mode. Switches between modes could also lead to problems, however. In congested airspace, an aircraft switching modes to follow a TCAS advisory could trigger a new conflict with a third aircraft, initiating a domino effect. Thus, careful analysis of safety under mode switching is necessary. A key focus of this effort will be on safety analysis of the described hybrid system model. Specifically, hybrid system reachability analysis will be used to determine conditions under which it is safe to switch from one mode to another.

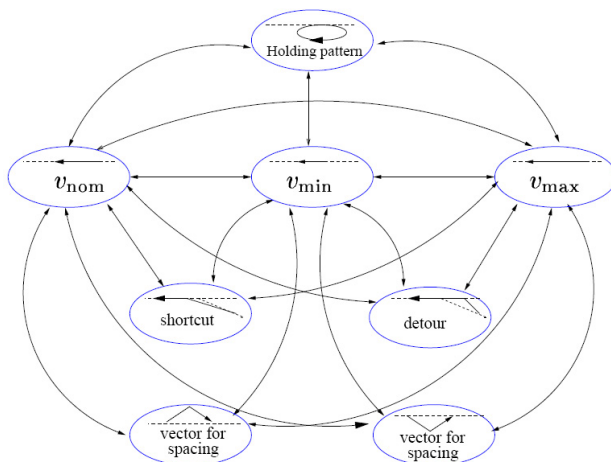


Figure 2. Hybrid system model of an aircraft in which the modes represent the ATC command. Very simple kinematics describe the motion of the aircraft in each mode. Figure courtesy of Professor Alexandre Bayen.

III. Safety Analysis: Methodology

Safety analysis of interacting collision avoidance schemes across the different layers of the hierarchy can be performed using reachable set computation for continuous and hybrid systems. Computing reachable sets is analogous to the development and execution of a mathematical proof that the system of aircraft involved in a conflict satisfies a safety property.

Computing reachable sets for a continuous or hybrid system may be used to answer the question: Do all trajectories of the system remain safe? To answer this question, one could first characterize the unsafe configurations of a system as a subset of the systems' state space. One could then compute all initial configurations of the system which could end up in one of those unsafe configurations. Then safety could be ensured by keeping the system out of these computed initial configurations. These initial configurations are known as the backwards reachable set of the given unsafe configurations.

Computing the backwards reachable set thus requires determining all initial states for which, for all possible control inputs, there exists a disturbance which could guide the system to an unsafe configuration. Previous work has shown that this backwards reachable set may be characterized as the zero sublevel sets of a particular Hamilton-Jacobi-Isaacs partial differential equation, encoding a game between control and disturbance. This work has also designed a procedure to compute this set for continuous and hybrid systems.^{16,17} For hybrid systems, the procedure calculates the subset of the continuous state space which is backward reachable from a defined unsafe subset of the continuous state space in each discrete mode of operation, and iterates this calculation through each switch between modes. Thus, the method effectively delineates the state space into safe and unsafe regions: as the system approaches the boundary of the unsafe region, corrective control action must be applied. This control action is computed automatically as part of the solution of the reachable set calculation.

The procedure to compute reachable sets for hybrid systems is based on the continuous state method, with allowances for discrete switches between modes. In the extension to hybrid systems, the reachable set computation involves an iterative process with a level set computation and a discrete switch at each step.¹⁶ The resulting reachable set may be used to extract the correct switching logic for the system: that is, given a range of possible switches between modes, the computation will indicate which of those switches are allowable in order to satisfy the control objective.

IV. Safety Analysis Between the Immediate and Midterm Schemes

To determine the safety of the interaction between the immediate and midterm schemes, both the lateral and the vertical reachable sets need to be evaluated.

A. Lateral Reachable Set

Previous work has already used the lateral reachable set to generate provably-safe conflict resolution maneuvers for aircraft in uncertain environments.¹⁸ For completeness, the problem formulation and solution will be repeated here. The relative coordinate system used for the aircraft is shown in Figure 3 and is attached to the evader. The model of each aircraft is based upon a kinematic model in which each aircraft has a fixed forward velocity, a heading angle, and a control input of angular velocity. In this scenario, a collision occurs if the two aircraft get within a distance r of each other. Since a collision only depends on the aircrafts' relative position, the problem can be solved in relative coordinates, which reduces the number of states. The relative dynamics of the two aircraft are given by:

$$\dot{x} = \frac{d}{dt} \begin{bmatrix} x_r \\ y_r \\ \psi_r \end{bmatrix} = \begin{bmatrix} -v + v \cos \psi_r + ay_r \\ v \sin \psi_r - ax_r \\ b - a \end{bmatrix} \quad (1)$$

where x_r and y_r are the relative position offsets of the two aircraft, ψ_r is the relative angular heading, v is the fixed linear velocity of each aircraft, $a \in \mathcal{A}$ is the angular velocity of the evader, and $b \in \mathcal{B}$ is the angular velocity of the pursuer.

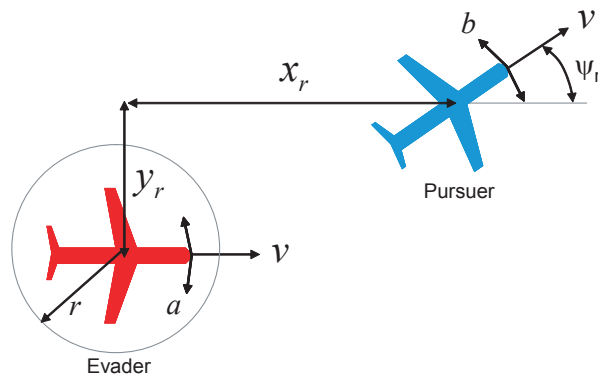


Figure 3. Relative coordinate system for the two aircraft, used in the lateral reachable set calculation.

Figure 4 shows the backwards reachable set, calculated by using Ian Mitchell's Toolbox of Level Set Methods,¹⁹ with $v = 774 \text{ ft/s}$, $\mathcal{A} = \mathcal{B} = [-15 \ 15]^\circ \text{ sec}^{-1}$, and $r = 0.1 \text{ nmi}$. The vertical axis is the relative heading angle between the aircraft and each horizontal slice represents all possible relative position offsets of the aircraft for a fixed relative heading. The most extended part of the helical bulge occurs for $\psi_r = \pi$. This is intuitive because in this scenario the aircraft are flying directly at each other, resulting in the largest region of unsafe initial conditions. Also, the backwards reachable set is the smallest at the top and bottom, which corresponds to the aircraft flying in the same direction. The backwards reachable set ceases to grow after approximately 5 seconds at which time the pursuer no longer has any action which can capture the evader. Therefore, if the evader's and pursuer's initial conditions are outside of the backwards reachable set, then there exists a control input for the evader that will avoid a collision regardless of the pursuer's input.

B. Vertical Reachable Set

Since the lateral reachable set only considers possible collisions in 2D, the vertical direction also needs to be considered.

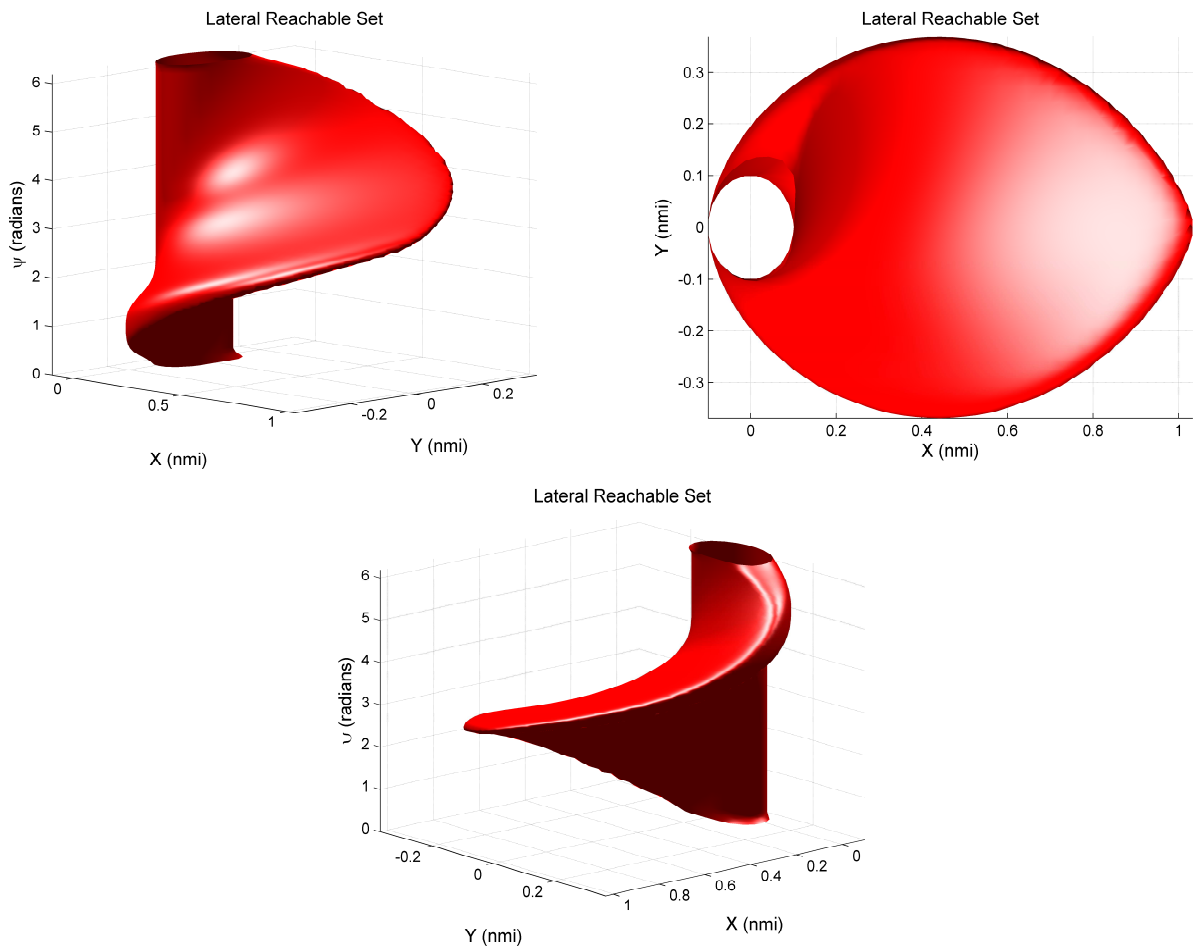


Figure 4. Several views of the lateral reachable set with initial conditions of $r = 0.1$ nautical miles. The vertical axis is the relative heading angle between the aircraft and a horizontal slice represents all possible relative position offsets of the aircraft for a fixed relative heading. If the pursuer starts anywhere inside the reachable set, a collision can occur regardless of any input the evader may choose. Conversely, if the pursuer starts outside of the reachable set, then there exists a control input for the evader that will avoid a collision regardless of the pursuer's input.

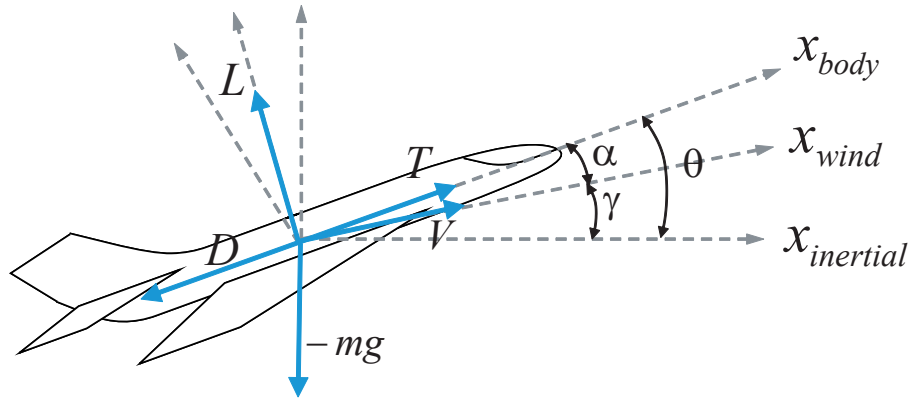


Figure 5. Point mass force diagram for the longitudinal dynamics of the aircraft.

1. Longitudinal Dynamics

The point mass model of the longitudinal dynamics of an aircraft is shown in Equation (2) which refers to Figure 5. Each aircraft has 3 states: the magnitude of the velocity (V), the angle of the wind vector (γ), and the Z position (altitude) of the aircraft. Each aircraft has two inputs which correspond to the thrust (T) and angle of attack (α).

$$\frac{d}{dt} \begin{bmatrix} V \\ \gamma \\ Z \end{bmatrix} = \begin{bmatrix} \frac{1}{m} (T \cos \alpha - D(\alpha, V) - mg \sin \gamma) \\ \frac{1}{mV} (T \sin \alpha + L(\alpha, V) - mg \cos \gamma) \\ V \sin \gamma \end{bmatrix} \quad (2)$$

The Lift and Drag are given by:

$$\begin{aligned} D(\alpha, V) &= \frac{1}{2} \rho S V^2 C_D \\ L(\alpha, V) &= \frac{1}{2} \rho S V^2 C_L(\alpha) \end{aligned} \quad (3)$$

The dimensionless lift and drag coefficients are:

$$\begin{aligned} C_L(\alpha) &= C_{L_0} + C_{L_\alpha} \alpha \\ C_D &= C_{D_0} + K C_L(\alpha)^2 \end{aligned} \quad (4)$$

Since reachable set analysis is very computationally intensive, the dynamics were simplified for each aircraft so that the calculations become tractable. The simplification used is to assume that the magnitude of the velocity is constant and that the thrust is used to maintain the velocity. Consequently, each aircraft will only have one input which corresponds to the angle between the velocity vector and the aircraft (α). Although this might be a restrictive simplification, if a potentially unsafe state can be found using reachable set analysis on the simplified model, then it will indicate where a problem might exist with the actual system and one can investigate it more closely. In these equations, subscript p and e are used for the pursuer and evader, respectively. With these simplifications, the relative dynamics of the two aircraft are given by

$$f_z(x, \alpha_e, \alpha_p) = \frac{d}{dt} \begin{bmatrix} \gamma_e \\ \gamma_p \\ Z_r \end{bmatrix} = \begin{bmatrix} \frac{1}{m_e V_e} (T_e \sin \alpha_e + L(\alpha_e, V_e) - m_e g \cos \gamma_e) \\ \frac{1}{m_p V_p} (T_p \sin \alpha_p + L(\alpha_p, V_p) - m_p g \cos \gamma_p) \\ V_p \sin \gamma_p - V_e \sin \gamma_e \end{bmatrix} \quad (5)$$

where the thrust for each aircraft is given by

$$T_i = \frac{1}{\cos \alpha_i} [D(\alpha_i, V_i) + m_i g \sin \gamma_i] \quad (6)$$

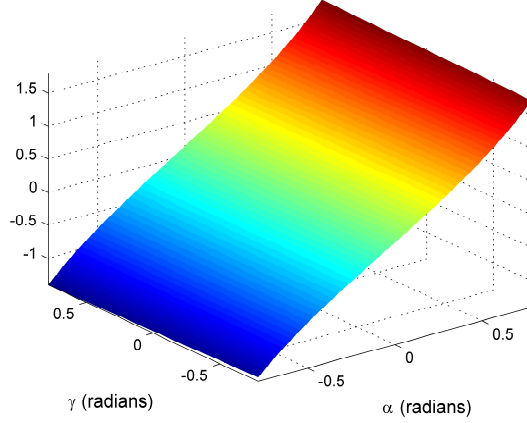


Figure 6. Optimized function from the Hamiltonian of the reachable set calculation.

2. Hamilton-Jacobi-Isaacs

To compute the reachable set, the Hamiltonian in Equation (7) needs to be evaluated, which entails finding the optimal inputs α_e^* and α_p^* .

$$H(x, p) = \max_{\alpha_e \in \mathcal{A}} \min_{\alpha_p \in \mathcal{B}} p^T f_z(x, \alpha_e, \alpha_p) \quad (7)$$

where $\mathcal{A} = [\mathcal{A}^{min}, \mathcal{A}^{max}]$, $\mathcal{B} = [\mathcal{B}^{min}, \mathcal{B}^{max}]$ and $p = [p_1 \ p_2]^T$ is the costate of the system. After simplification and combining terms:

$$\begin{aligned} p^T f_z(x, \alpha_e, \alpha_p) &= [p_3 (V_p \sin \gamma_p - V_e \sin \gamma_e) - p_1 mg \cos \gamma_e - p_2 mg \cos \gamma_p] + \\ & p_1 \left(\frac{1}{mV_e} [\tan \alpha_e (D(\alpha_e, V_e) + mg \sin \gamma_e) + L(\alpha_e, V_e)] \right) + \\ & p_2 \left(\frac{1}{mV_p} [\tan \alpha_p (D(\alpha_p, V_p) + mg \sin \gamma_p) + L(\alpha_p, V_p)] \right) \end{aligned} \quad (8)$$

Since the first term in Equation (8) does not depend on α_e or α_p , it can be neglected when evaluating the max and min operations. Also, the second and third terms only depend on α_e and α_p , respectively; therefore, the max and min operation decouple and can be considered separately. Consequently, the Hamiltonian in Equation (7) simplifies to

$$\begin{aligned} H(x, p) &= [p_3 (V_p \sin \gamma_p - V_e \sin \gamma_e) - p_1 mg \cos \gamma_e - p_2 mg \cos \gamma_p] + \\ & \max_{\alpha_e \in \mathcal{A}} p_1 \left(\frac{1}{mV_e} [\tan \alpha_e (D(\alpha_e, V_e) + mg \sin \gamma_e) + L(\alpha_e, V_e)] \right) + \\ & \min_{\alpha_p \in \mathcal{B}} p_2 \left(\frac{1}{mV_p} [\tan \alpha_p (D(\alpha_p, V_p) + mg \sin \gamma_p) + L(\alpha_p, V_p)] \right) \end{aligned} \quad (9)$$

The function that is minimized/maximized is the same in each case and is shown in Figure 6. The parameters used for the plot are the same that are used for the simulations in the following section. As shown in Figure 6, the function has its maximum and minimum at its endpoints. Therefore the optimal inputs are:

$$\begin{aligned} \alpha_e^* &= \begin{cases} \mathcal{A}^{min} & \text{if } p_1 < 0 \\ \mathcal{A}^{max} & \text{otherwise} \end{cases} \\ \alpha_p^* &= \begin{cases} \mathcal{B}^{min} & \text{if } p_2 > 0 \\ \mathcal{B}^{max} & \text{otherwise} \end{cases} \end{aligned} \quad (10)$$

These optimal inputs can be used to compute now be used to compute the backwards reachable set.

3. Results

Figure 7 shows the backwards reachable set for vertical separation. The initial conditions for the aircraft is a vertical separation of $Z_r = 500$ feet, with $\pm Z_r$ corresponding to the two possible relative positions of the aircraft. These two possible initial conditions are represented by the blue planes in Figure 7. The realistic operating conditions that are imposed on the aircraft are $\gamma \in [-45^\circ, 45^\circ]$. Both aircraft are assumed to be identical with the following parameters:

$$\begin{aligned}
 V &= 774 & \text{ft/sec} & & C_{L\alpha} &= 5.105 \\
 m &= 13019.14 & \text{slugs} & & K &= 0.04831 \\
 g &= 32.2 & \text{ft/sec}^2 & & C_{D0} &= 0.025 \\
 \rho &= 0.002377 & \text{slug/ft}^3 & & S &= 4596.19 \text{ ft}^2 \\
 C_{Lo} &= 0.4225
 \end{aligned}$$

For this example, the evader's and pursuer's input range is $\mathcal{A} = \mathcal{B} = [-15, 15]^\circ \text{sec}^{-1}$. The reachable set in the positive Z direction grows larger than in the negative direction, which is caused by the effect of gravity on the pursuer when it is below the evader. Also, for $Z_r > 0$, the reachable set does not grow for $\gamma_e \leq \gamma_p$, corresponding to $\dot{Z}_r(0) \geq 0$, because there is no input for the pursuer to enter the evader's "restricted" airspace since the control input range is the same for both. Also, the backwards reachable set grows the largest when the aircraft are pointing toward each other, which occurs for $\gamma_e = -\gamma_p = \pm\pi/4$.

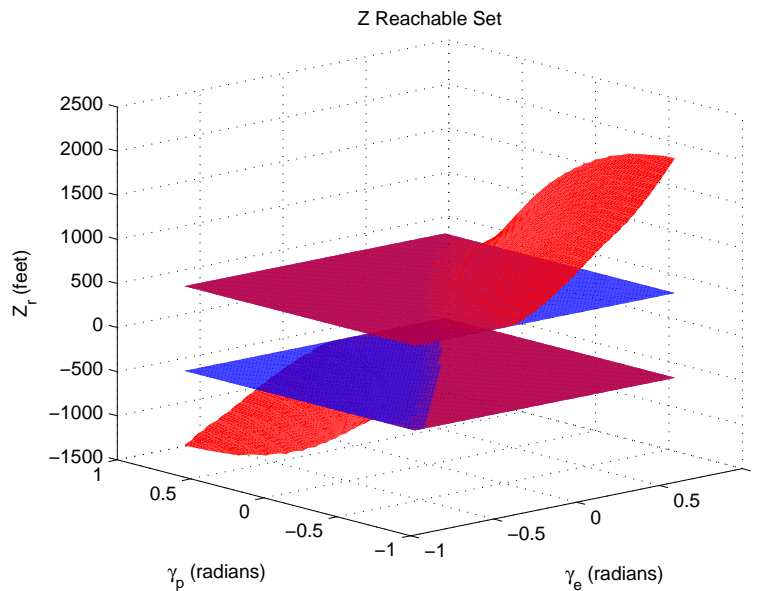


Figure 7. Vertical Reachable Set. The initial conditions, which are two infinite planes at ± 500 feet, are shown in blue and the backwards reachable set is shown in red. Intuitively, the backwards reachable set grows the largest when the aircraft are pointing toward each other, which occurs for $\gamma_e = -\gamma_p = \pm\pi/4$.

C. Conclusions

The method of using two independent reachable sets for determining safe initial conditions is conservative because in actuality the lateral and longitudinal dynamics are not independent. One dependency occurs in the X position of the aircraft between the two different dynamic models. Although the two dynamic models are inconsistent when used together, since they provide a conservative over-approximation of the reachable set, safety can still be guaranteed. If the initial conditions for the two aircraft are outside of either reachable set, then there exists a control input for the evader to avoid a mid-air collision. Therefore, for any arbitrary immediate collision avoidance scheme, if the midterm scheme keeps all trajectories outside of either the

lateral or vertical backwards reachable set then the evader has an action to maintain safety.

These conditions are necessary but not sufficient to guarantee safety between the immediate and midterm collision avoidance algorithms, for all immediate collision avoidance schemes. Not all immediate collision avoidance schemes will apply the optimal inputs to maintain aircraft safety which is assumed in the reachable set analysis. Each immediate collision avoidance scheme must be analyzed separately to determine all initial conditions in which it cannot prevent a collision. Once these are found, they must be included with the previous two reachable sets as the initial conditions for the backwards reachable set for the midterm collision avoidance scheme. Then these initial conditions will encompass all states in which the midterm scheme must stay out of in order to guarantee the safety of the interaction between the immediate and midterm collision avoidance schemes.

V. Traffic Alert and Collision Avoidance System

A. TCAS Alert System

Today, TCAS is installed on all commercial aircraft with at least 19 passenger seats, operating in the US.^{5,20,21} It receives and displays bearing and relative altitude information about all other aircraft within a 40 mile radius, and provides traffic alerts and a resolution advisory (climb or descend command) to resolve near mid-air collisions.²¹

TCAS performs range and altitude tests in order to analyze the situation between the two aircraft. TCAS uses the time-to-go to the closest point of approach, referred to as τ , to determine whether or not an aircraft is a threat. If the rate of closure is very low, it will use a minimum range, referred as DMOD, to avoid the aircraft becoming very close but not triggering the alert.²¹ The range test criteria²² is:

$$Range_Test_{ij} = \left((\dot{R}_{ij} > RDTHR) \wedge \hat{R}_1 \right) \vee \left((\dot{R}_{ij} \leq RDTHR) \wedge \hat{R}_2 \right) \quad (11)$$

with

$$\hat{R}_1 = (R_{ij} \leq DMOD) \wedge (R_{ij} \dot{R}_{ij} \leq H_1) \quad (12)$$

and

$$\hat{R}_2 = (R_{ij} \leq RMAX) \wedge \left(\frac{R_{ij} - \frac{DMOD^2}{R_{ij}}}{\min \{ \dot{R}_{ij}, -RDTHR \}} < TRTHR \right) \quad (13)$$

R_{ij} is the range between the two aircraft. RMAX and RDTHR are system constants with values of 12 nmi and 10 ft/s, respectively. DMOD is the distance modification or minimum range with units of nmi, H_1 is the threat minimum divergence threshold with units of nmi²/s, and TRTHR is the modified τ threshold with units of seconds; these system parameters vary with the altitude of the aircraft and with the sensitivity level set by the pilot.

The altitude resolution logic will estimate the vertical separation at the time of closest point of approach. If the vertical separation is below an altitude threshold, which depends upon the altitude, it will satisfy the vertical test for issuing an alert:²²

$$Altitude_Test = \left| \Delta h - \Delta \dot{h} \tau \right| \leq Z_{threshold} \quad (14)$$

In order for the aircraft to be declared as a threat, the aircraft needs to satisfy the range test as well as the altitude test. In practice, even if both of the criteria are satisfied, TCAS may not issue an alert to avoid false alarms.

B. Reachable Sets for TCAS

The vertical reachable set that is calculated is a two player game in which the pursuer is trying to enter the evader's restricted airspace. Since the pursuer is not helping the evader maintain separation, safety of

the aircraft can be guaranteed even if the pursuer does not follow its resolution advisory. In the perfect TCAS scenario, the two aircraft would be working together to maintain separation; therefore the reachable set calculated is conservative.

In order to ensure safety of the two aircraft, pilot delay was also included into the backwards reachable set, which is shown in Figure 8. To incorporate pilot delay, the true backwards reachable set was calculated and used as the initial conditions for the reachable set calculation using no control input for t_{delay} .

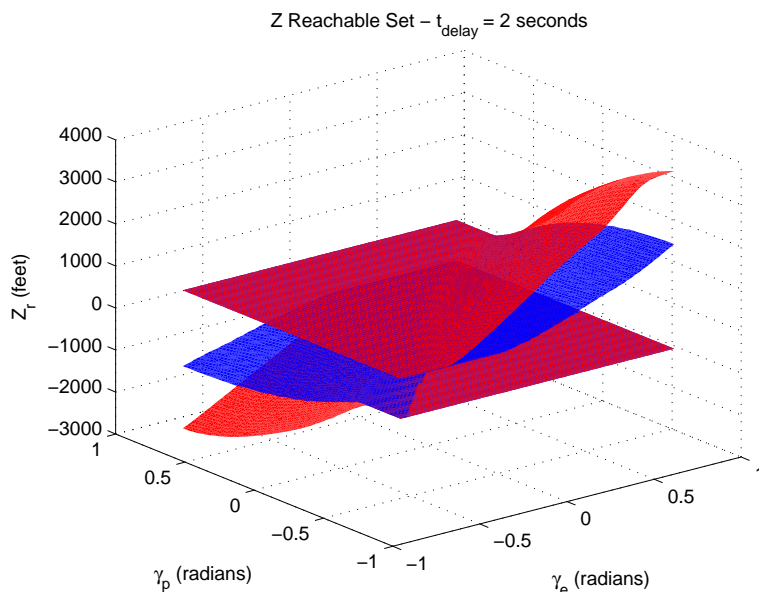


Figure 8. Vertical reachable set with a pilot delay incorporated. A two second pilot delay appended onto the backwards reachable set is shown in red with the original backwards reachable set shown in blue.

Figure 9 shows a comparison between two reachable sets with two different ranges of control input for the evader and pursuer. As the figure shows, a decrease in control authority directly causes an increase in the size of the backwards reachable set. Figure 10 superimposes the TCAS vertical alert on top of the two second pilot delay backwards reachable set for the two different control input ranges. For Figure 10(a), the TCAS alert is issued outside of the backwards reachable set which means that in this scenario TCAS should maintain the safety of the aircraft (if the pilot delay isn't too large). In Figure 10(b), the TCAS alert is not completely outside of the reachable set, which means that there could be cases in which the aircraft collide. The portion of the TCAS alert set which is inside of the reachable set corresponds to high vertical rates. A study by Lincoln labs²⁰ performed a series of simulations to evaluate the performance of TCAS. In this study, as expected from this analysis, they found that for certain instances with high vertical rates TCAS could not resolve the conflict.

VI. Conclusions and Future Work

In summary, a modeling framework was introduced for analyzing tiered collision avoidance schemes and determining if the interaction between the individual collision avoidance regimes will maintain the safety of the national airspace. The transition between the immediate and midterm schemes was also analyzed, and provable safety conditions were provided. The immediate collision avoidance scheme, TCAS, was also analyzed independently to show that for certain parameters and circumstances TCAS could be unsafe and not able to resolve near mid-air collisions.

In future work, the authors plan on combining the reachable set analysis with a simulator of the TCAS algorithm to determine unsafe initial conditions for the TCAS algorithm. This will provide the additional unsafe initial conditions specific to TCAS for the backwards reachable set of the midterm collision avoidance

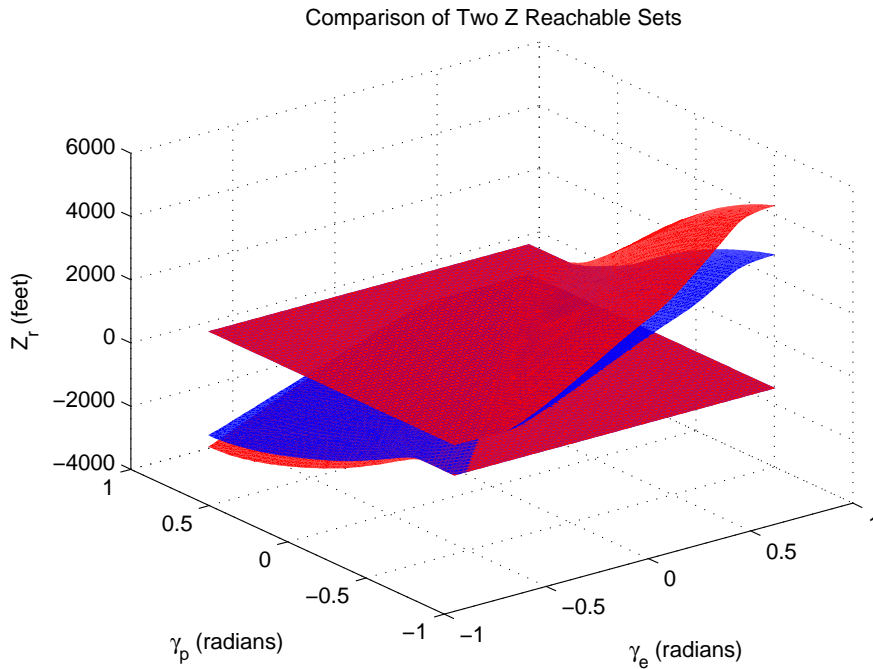


Figure 9. A comparison of the backwards reachable set with the evader's control input bounded by $\mathcal{A} = \mathcal{B} = [-15\ 15]^\circ\text{sec}^{-1}$ in blue and with the evader's control input bounded by $\mathcal{A} = \mathcal{B} = [-10^\circ/s\ 10^\circ/s]$ in red. A decrease in control authority directly causes an increase in the backwards reachable set.

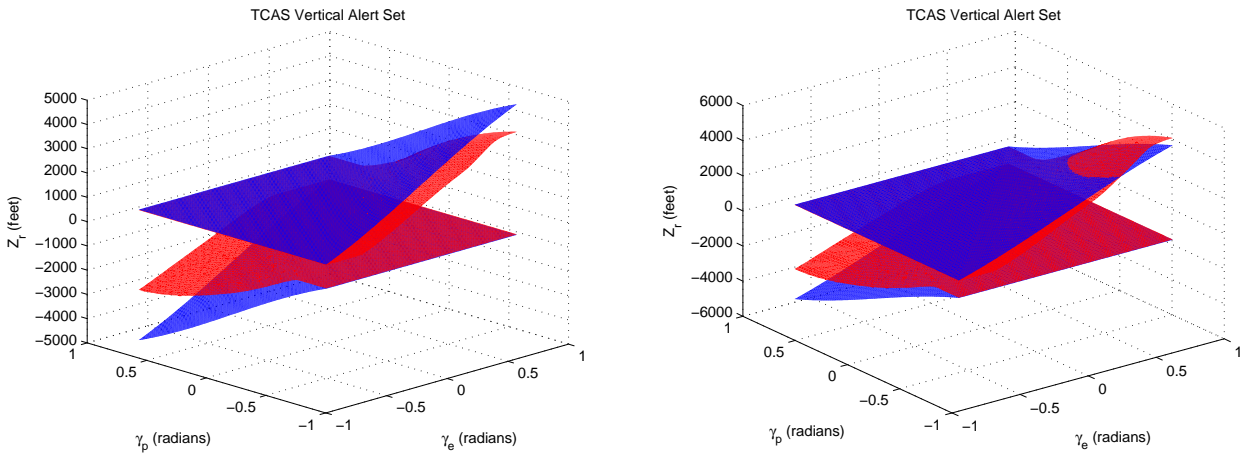


Figure 10. TCAS vertical alert set (blue) with the two second pilot delay reachable set (red). (a) Control input of the evader and pursuer is $\mathcal{A} = \mathcal{B} = [-15\ 15]^\circ\text{sec}^{-1}$. (b) Control input of the evader and pursuer is $\mathcal{A} = \mathcal{B} = [-10\ 10]^\circ\text{sec}^{-1}$. As shown, for the case in which the aircraft have less control authority, TCAS does not issue an alert in enough time to guarantee the safety of the aircraft.

scheme. Since in some situations more than two aircraft will be involved in a collision, the authors plan on also extending this work for multi-aircraft encounters.

References

- ¹Hu, J., Prandini, M., and Sastry, S., "Optimal coordinated maneuvers for three dimensional aircraft conflict resolution," *Journal of Guidance, Control, and Dynamics*, 2002, pp. 25(5):888–900.
- ²Frazzoli, E., Mao, Z. H., Oh, J. H., and Feron, E., "Aircraft conflict resolution via semidefinite programming," *AIAA Journal of Guidance, Control, and Dynamics*, 2001, pp. 24(1):79–86.
- ³Erzberger, H., "Automated conflict resolution for air traffic control," *In Proceedings of the 25th International Congress of the Aeronautical Sciences*, Germany, September 2006, pp. 437–457, To appear.
- ⁴Bilimoria, K., "A geometric optimization approach to aircraft conflict resolution," *In Proceedings of the AIAA Guidance, Navigation, and Control Conference*, August, Denver 2000, pp. AIAA 2000–4265.
- ⁵Harman, W. H., "TCAS: A system for preventing midair collisions," *The Lincoln Laboratory Journal*, 1989, pp. 437–457.
- ⁶Chen, Y.-B. and Inselberg, A., "Conflict resolution for air traffic control," Tech. Rep. USC-CS-93-543, Computer Science Department, University of Southern California, 1993.
- ⁷Hwang, I. and Tomlin, C. J., "Multiple aircraft conflict resolution under finite information horizon," *In Proceedings of the American Control Conference*, Anchorage, AL, May 2002.
- ⁸Dowek, G., Geser, A., , and Muñoz, C., Tech. Rep. 2001-7, NASA/CR-2001-210853 ICASE, 2001.
- ⁹Zhao, Y. and Schultz, R., "Deterministic resolution of two aircraft conflict in free flight," *In Proceedings of the AIAA Guidance, Navigation and Control Conference*, August, New Orleans, LA 1997, pp. AIAA–97–3547.
- ¹⁰Krozel, J., Mueller, T., and Hunter, G., "Free flight conflict detection and resolution analysis," *In Proceedings of the AIAA Guidance, Navigation and Control Conference*, San Diego, CA, August 1996.
- ¹¹Košec̆ka, J., Tomlin, C., Pappas, G., and Sastry, S., "2-1/2D conflict resolution maneuvers for ATMS," *In Proceedings of the IEEE Conference on Decision and Control*, Tampa, FL, 1998, pp. 2650–2655.
- ¹²Tomlin, C. J., *Hybrid Control of Air Traffic Management Systems*, Ph.D. thesis, Department of Electrical Engineering, University of California, Berkeley, 1998.
- ¹³Alur, R. and Dill, D., "A theory of timed automata," *Theoretical Computer Science*, 1994, pp. 183–235.
- ¹⁴Bayen, A. M., Grieder, P., Sipma, H., Tomlin, C. J., and Meyer, G., "Delay predictive models of the National Airspace System using hybrid control theory," *In Proceedings of the American Control Conference*, Anchorage, AL, May 2002, pp. 767–772.
- ¹⁵Bayen, A. M., *Computational Control of Networks of Dynamical Systems: Application to the National Airspace System*, Ph.D. thesis, Aeronautics and Astronautics, Stanford University, December 2003.
- ¹⁶Tomlin, C. J., Lygeros, J., and Sastry, S., "A game theoretic approach to controller design for hybrid systems," *In Proceedings of the IEEE*, July 2000, pp. 949–970.
- ¹⁷Mitchell, I. M., Bayen, A. M., and Tomlin, C. J., "A Time-Dependent Hamilton-Jacobi Formulation of Reachable Sets for Continuous Dynamic Games," *IEEE Transactions on Automatic Control*, July 2005, pp. 947–957.
- ¹⁸Tomlin, C., Mitchell, I., and Ghosh, R., "Safety Verification of Conflict Resolution Maneuvers," *IEEE Transactions on Intelligent Transportation Systems*, Vol. 2, June 2001.
- ¹⁹Mitchell, I. M., "The Flexible, Extensible and Efficient Toolbox of Level Set Methods." *Journal of Scientific Computing*, December 2007.
- ²⁰Drumm, A., "Lincoln laboratory evaluation of TCAS II logic version 6.04a," Tech. Rep. ATC-240, Lincoln Laboratory, MIT, 1996.
- ²¹Administration, F. A., "Introduction to TCAS II, Version 7," November 2000.
- ²²Livadas, C., Lygeros, J., and Lynch, N. A., "High-Level Modeling and Analysis of the Traffic Alert and Collision Avoidance System (TCAS)," *In Proceedings of the IEEE*, 2000.